The Canadian Mineralogist
Vol. 43, pp. 1501-1510 (2005)

OXYKINOSHITALITE, A NEW SPECIES OF MICA FROM FERNANDO DE NORONHA ISLAND, PERNAMBUCO, BRAZIL: OCCURRENCE AND CRYSTAL STRUCTURE

LIA N. KOGARKO

Vernadsky Institute of Geochemistry, Russian Academy of Sciences, Kosygin Street 19, Moscow 119991, Russia

YULIA A. UVAROVA, ELENA SOKOLOVA[§] AND FRANK C. HAWTHORNE

Department of Geological Sciences, University of Manitoba, Winnipeg, Manitoba R3T 2N2, Canada

LUISA OTTOLINI

Istituto di Geoscienze e Georisorse (IGG), Sezione di Pavia, via Ferrata, 1, I–27100 Pavia, Italy

JOEL D. GRICE

Research Division, Canadian Museum of Nature, P.O. Box 3443, Station D, Ottawa, Ontario K1P 6P4, Canada

ABSTRACT

Oxykinoshitalite, ideally Ba (Mg_2 Ti^{4+}) (Si_2 Al_2) O_{10} O_2, is a new species of mica from Fernando de Noronha Island, Pernambuco, Brazil; it is found in an olivine nephelinite with olivine, clinopyroxene, Fe–Ti oxide, nepheline, calcite, apatite and K-rich feldspar. Oxykinoshitalite forms corroded irregularly shaped grains 0.03 to 0.05 mm across, and its color varies from bright orange to brown. It is brittle, $H = 2½$, $D_{obs} = 3.3(1)$, $D_{calc} = 3.45$ g/cm^3, has a brown streak, vitreous luster and does not fluoresce in ultraviolet light; it has a perfect cleavage on {001} and a splintery fracture. In transmitted plane-polarized light, oxykinoshitalite is strongly pleochroic, X pale brown, $Y \approx Z$ deep red-brown; $X \wedge c = 2°$ (in β obtuse), $Y = b$, $Z \wedge a = 8°$ (in β obtuse), with absorption $X < Y \approx Z$. It is biaxial positive, α 1.708 ± 0.001, β 1.710 ± 0.001, γ 1.719 ± 0.001, $2V_{obs} = 56 \pm 2°$, $2V_{calc} = 51°$. Oxykinoshitalite is monoclinic, space group $C2/m$, a 5.3516(7), b 9.2817(11), c 10.0475(13) Å, β 100.337(3)°, V 490.98(18) Å^3, $Z = 2$. The strongest ten X-ray-diffraction lines in the powder pattern [d in Å(I)(hkl)] are: 2.637(10)($\bar{1}31$), 2.172(9)($\bar{1}33$), 3.646(7)($\bar{1}12$), 3.130(7)(112), 3.383(6)(002), 2.902(5)($\bar{1}13$), 2.435(5)(201), 1.988(5)(133), 1.661(5)($\bar{1}35$), 1.547(5)(312), and 1.526(5)($\bar{2}06$). Analysis by a combination of electron microprobe, SIMS and crystal-structure refinement gives SiO_2 28.92, Al_2O_3 15.26, TiO_2 11.94, Cr_2O_3 0.03, Fe_2O_3 9.07, FeO 3.84, MnO 0.14, MgO 10.74, CaO 0.03, BaO 15.49, Na_2O 0.39, K_2O 4.05, F 0.91, H_2O 0.55, sum 100.97 wt.%; V, Ni, Zn, Sr, Cl were not detected. The formula unit, calculated on the basis of 12(O,OH,F) is $(Ba_{0.50}\ K_{0.43}\ Na_{0.07})_{\Sigma 1.00}$ $(Mg_{1.33}\ Fe^{2+}_{0.27}\ Mn^{2+}_{0.01}\ Fe^{3+}_{0.57}\ Ti^{4+}_{0.74})_{\Sigma 2.92}$ $(Si_{2.40}\ Al_{1.49})_{\Sigma 3.89}$ O_{10} $[O_{1.46}\ (OH)_{0.30}\ F_{0.24}]_{\Sigma 2.00}$. Refinement of the crystal structure shows it to be the $1M$ polytype. The refinement converged to $R_1 = 4.3\%$ for 585 unique ($F_o > 4\sigma F_o$) reflections, collected on a Bruker single-crystal $P4$ diffractometer with a CCD detector and Mo$K\alpha$ X-radiation. Electron-microprobe and SIMS analysis of the crystal used to collect the data on X-ray intensities gave the empirical formula $(Ba_{0.47}\ K_{0.42}\ Na_{0.06}\ Ca_{0.01})_{\Sigma 0.96}$ $(Mg_{1.35}\ Fe^{2+}_{0.28}\ Fe^{3+}_{0.59}\ Ti^{4+}_{0.75}\ Mn_{0.01})_{\Sigma 2.98}$ $[Si_{2.31}\ Al_{1.56}]_{\Sigma 3.97}$ O_{10} $(O_{1.44}\ OH_{0.31}\ F_{0.25})_{\Sigma 2.00}$. The oxygenian Ti-dominant analogue of kinoshitalite occurs in olivine nephelinite and is associated with olivine, clinopyroxene, Fe–Ti oxide, nepheline, calcite, apatite and K-rich feldspar. There is one tetrahedrally coordinated T site, $\langle T\text{–O}\rangle = 1.671$ Å, occupied by $(Si_{2.31}\ Al_{1.56})$. There are two octahedrally coordinated sites, $M(1)$ occupied by $(Mg_{0.52}\ Fe^{2+}_{0.13}\ Fe^{3+}_{0.27}\ Ti^{4+}_{0.08})$ with $\langle M(1)\text{–O}\rangle = 2.110$ Å, and $M(2)$ occupied by $(Mg_{0.84}\ Fe^{2+}_{0.15}\ Fe^{3+}_{0.33}\ Mn_{0.01}\ Ti^{4+}_{0.67})$ with $\langle M(2)\text{–O}\rangle = 2.065$ Å. The interstitial [12]-coordinated I site is occupied by $(Ba_{0.47}\ K_{0.42}\ Na_{0.06}\ Ca_{0.01})$, with $\langle I\text{–O}\rangle = 3.107$ Å. There are two main coupled substitutions in this structure: (1) Ti^{4+} for Mg, primarily at the $M(2)$ site, and O^{2-} for $(OH)^-$ and F^- at the O(4) site, and (2) K for Ba at the I site, and Si for Al at the T site.

Keywords: oxykinoshitalite, new mineral species, crystal-structure refinement, oxygenian mica, Fernando de Noronha Island, Brazil.

[§] *E-mail address*: elena_sokolova@umanitoba.ca

SOMMAIRE

Nous décrivons l'oxykinoshitalite, de composition idéale $Ba (Mg_2 Ti^{4+}) (Si_2 Al_2) O_{10} O_2$, une nouvelle espèce de mica provenant de l'île de Fernando de Noronha, au Brésil; on la trouve dans une néphélinite à olivine, associée à olivine, clinopyroxène, oxyde Fe–Ti, néphéline, calcite, apatite et feldspath potassique. L'oxykinoshitalite se présente en cristaux xénomorphes d'aspect corrodé de 0.03 à 0.05 mm de diamètre. Sa couleur varie d'orange vif à brun. C'est un minéral cassant, d'une dureté de 2½; sa densité observée est 3.3(1), et sa densité calculée, 3.45 g/cm^3. Il a une rayure brune, un éclat vitreux, et ne montre aucune fluorescence en lumière ultra-violette. Il a un clivage parfait sur {001} et une fracture en esquilles. En lumière transmise polarisée, l'oxykinoshitalite est fortement pléochroïque, X brun pâle, $Y \approx Z$ brun rougeâtre foncé, $X \wedge c = 2°$ (dans l'angle β obtus), $Y = b$, $Z \wedge a = 8°$ (dans l'angle β obtus), avec absorption $X < Y \approx Z$. Elle est biaxe positive, α 1.708 ± 0.001, β 1.710 ± 0.001, γ 1.719 ± 0.001, $2V_{obs} = 56 \pm 2°$, $2V_{calc} = 51°$. L'oxykinoshitalite est monoclinique, groupe spatial $C2/m$, a 5.3516(7), b 9.2817(11), c 10.0475(13) Å, β 100.337(3)°, V 490.98(18) Å^3, $Z = 2$. Les dix raies les plus intenses en diffraction X (méthode des poudres) [d en Å(I)(hkl)] sont: 2.637(10)($\bar{1}31$), 2.172(9)($\bar{1}33$), 3.646(7)($\bar{1}12$), 3.130(7)(112), 3.383(6)(002), 2.902(5)($\bar{1}13$), 2.435(5)(201), 1.988(5)(133), 1.661(5)($\bar{1}35$), 1.547(5)(312), et 1.526(5)($\bar{2}06$). Des analyses au moyen d'une microsonde électronique, microsonde ionique et les résultats de l'affinement de la structure ont donné SiO_2 28.92, Al_2O_3 15.26, TiO_2 11.94, Cr_2O_3 0.03, Fe_2O_3 9.07, FeO 3.84, MnO 0.14, MgO 10.74, CaO 0.03, BaO 15.49, Na_2O 0.39, K_2O 4.05, F 0.91, H_2O 0.55, pour un total de 100.97% (poids); nous n'avons pas décelé V, Ni, Zn, Sr et Cl. La formule unitaire, calculée sur une base de 12(O,OH,F), est $(Ba_{0.50} K_{0.43} Na_{0.07})_{\Sigma 1.00} (Mg_{1.33} Fe^{2+}_{0.27} Mn^{2+}_{0.01} Fe^{3+}_{0.57} Ti^{4+}_{0.74})_{\Sigma 2.92} (Si_{2.40} Al_{1.49})_{\Sigma 3.89} O_{10} [O_{1.46} (OH)_{0.30} F_{0.24}]_{\Sigma 2.00}$. L'affinement de la structure montre qu'il s'agit du polytype 1M. L'affinement a atteint un résidu de $R_1 = 4.3\%$ en utilisant 585 réflexions uniques ($F_o > 4\sigma F_o$), prélevées avec un diffractomètre Bruker P4 muni d'un détecteur CCD et utilisé avec rayonnement Mo$K\alpha$. Les résultats des analyses avec les microsondes électronique et ionique du cristal utilisé pour l'étude de la structure mènent à la formule empirique $(Ba_{0.47} K_{0.42} Na_{0.06} Ca_{0.01})_{\Sigma 0.96} (Mg_{1.35} Fe^{2+}_{0.28} Fe^{3+}_{0.59} Ti^{4+}_{0.75} Mn_{0.01})_{\Sigma 2.98} [Si_{2.31} Al_{1.56}]_{\Sigma 3.97} O_{10} (O_{1.44} OH_{0.31} F_{0.25})_{\Sigma 2.00}$. Cet analogue oxygéné à dominance de Ti de la kinoshitalite a été découvert dans une néphélinite à olivine; elle est associée à olivine, clinopyroxène, oxyde à Fe–Ti, néphéline, calcite, apatite et feldspath potassique. Il y a un site tétraédrique, $\langle T\text{–}O\rangle = 1.671$ Å, dont l'occupation est $(Si_{2.31} Al_{1.56})$. Il y a deux sites à coordinence octaédrique, $M(1)$, avec $(Mg_{0.52} Fe^{2+}_{0.13} Fe^{3+}_{0.27} Ti^{4+}_{0.08})$ et $\langle M(1)\text{–}O\rangle = 2.110$ Å, et $M(2)$, avec $(Mg_{0.84} Fe^{2+}_{0.15} Fe^{3+}_{0.33} Mn_{0.01} Ti^{4+}_{0.67})$ et $\langle M(2)\text{–}O\rangle = 2.065$ Å. Le site interstitiel I à coordinence [12] contient $(Ba_{0.47} K_{0.42} Na_{0.06} Ca_{0.01})$, avec $\langle I\text{–}O\rangle = 3.107$ Å. Il y a deux substitutions couplées dans cette structure: (1) Ti^{4+} pour Mg, impliquant surtout le site $M(2)$, et O^{2-} pour $(OH)^-$ et F^- au site O(4), et (2) Ba pour K au site I, et Si pour Al au site T.

(Traduit par la Rédaction)

Mots-clés: oxykinoshitalite, nouvelle espèce minérale, affinement de la structure cristalline, mica sur-oxygéné, île de Fernando de Noronha, Brésil.

INTRODUCTION

There are five accredited micas containing essential Ba: chernykhite, $Ba V_2 Al_2 Si_2 O_{10} (OH)_2$ (Ankinovich *et al.* 1973), anandite, $Ba Fe^{2+}_3 Fe^{3+} Si_3 O_{10} S (OH)$ (Pattiaratchi *et al.* 1967), kinoshitalite, $Ba Mg_3 Al_2 Si_2 O_{10} (OH)_2$ (Yoshii *et al.* 1973a), ferrokinoshitalite, $Ba Fe_3 Al_2 Si_2 O_{10} (OH)_2$ (Guggenheim & Frimmel 1999), and ganterite, $[Ba_{0.5} (Na,K)_{0.5}] Al_2 (Si_{2.5} Al_{1.5} O_{10}) (OH)_2$ (Graeser *et al.* 2003). In addition, several micas are enriched in Ba, *e.g.*, biotite, phlogopite, muscovite (Mansker *et al.* 1979, Wendlandt 1977, Gaspar & Wyllie 1982, Hetherington *et al.* 2003).

Kinoshitalite, ideally $Ba Mg_3 Al_2 Si_2 O_{10} (OH)_2$, was first described from the Noda–Tamagawa mine, Iwate Prefecture, Japan, in association with hausmannite, tephroite, celsian, quartz, spessartine, rhodonite, chalcopyrite and pyrrhotite (Yoshii *et al.* 1973a). The crystal structures of two samples of kinoshitalite-1M have been refined: $(Ba_{0.584} K_{0.352} Na_{0.110} Ca_{0.005})_{\Sigma 1.051} (Mg_{2.065} Mn^{2+}_{0.522} Al_{0.223} Mn^{3+}_{0.206} Fe^{2+}_{0.045} Fe^{3+}_{0.003})_{\Sigma 3.064} [Si_{2.052} Al_{1.938} Ti_{0.010}] O_{10.33} (OH_{1.615} F_{0.055})$, R_1 7.2%, a 5.345(3), b 9.250(4), c 10.256(8) Å, β 99.99(5)°, V 499.2 Å^3, $C2/m$ (Kato *et al.* 1979), and $(Ba_{0.54} K_{0.41} Na_{0.04} Ca_{0.01})_{\Sigma 1.00} (Mg_{2.53} Fe^{2+}_{0.27} Al_{0.17} Ti_{0.03})_{\Sigma 3.00} (Si_{2.17} Al_{1.83}) O_{9.94} F_{0.71} (OH)_{1.35}$, R_1 2.5%, a 5.318(1), b 9.214(1), c 10.164(1) Å, β 100.11(1)°, V 490.3 Å^3, $C2/m$ (Brigatti & Poppi 1993). In addition, McCauley & Newnham (1973) refined the structure of synthetic lithian fluorine-dominant analogue of kinoshitalite: $Ba_{0.97} (Mg_{2.23} Li_{0.77})(Si_{2.84} Al_{1.16}) O_{9.9} F_{2.08}$, R_1 7.1%, a 5.2858(2), b 9.1575(6), c 10.0375(5) Å, β 100.124(4)°, V 478.3 Å^3, $C2/m$. Guggenheim & Kato (1984) refined the crystal structure of kinoshitalite in the subgroups $C2$, Cm and $C\bar{1}$ and confirmed the space group $C2/m$ proposed by Kato *et al.* (1979). Usually, kinoshitalite has high contents of BaO and MnO and relatively low contents of FeO, Fe_2O_3 and TiO_2 (Kato *et al.* 1979, Dasgupta *et al.* 1989, Gnos & Armbruster 2000). Only one occurrence of Mn-poor kinoshitalite has been reported (Solie & Su 1987): $(Ba_{0.55} K_{0.40} Na_{0.03}) (Mg_{2.57} Al_{0.16} Fe^{2+}_{0.23} Fe^{3+}_{0.04} Ti_{0.01}) [Si_{2.24} Al_{1.76}] O_{10.00} (OH_{1.30} F_{0.70})$.

Ferrokinoshitalite occurs in massive Pb–Zn–Cu–Ag sulfide orebodies at the Broken Hill mine, northern Cape Province, South Africa. Associated minerals are quartz + magnetite + spessartine-rich garnet + apatite ± sillimanite ± ferroan gahnite ± sulfides, Mn-rich grunerite, manganoan fayalite and Mn-rich pyroxferroite (Guggenheim & Frimmel 1999). The crystal structure of ferrokinoshitalite, $(Ba_{0.47}\ K_{0.33}\ Na_{0.04})$ $(Fe^{2+}_{1.72}\ Mg_{0.74}\ Mn^{2+}_{0.08}\ Fe^{3+}_{0.15}\ Ti_{0.17})$ $[Si_{2.44}\ Al_{1.56}]$ $O_{10}\ (OH_{1.35}\ F_{0.65})$, monoclinic, $C2/m$, a 5.389(1), b 9.337(2), c 10.054(2) Å, β 100.53(2)°, was refined to a R_1 of 3.2% (Guggenheim & Frimmel 1999).

Here, we report the occurrence and crystal structure of Ti-rich oxykinoshitalite, a new species of mica from Fernando de Noronha Island, Brazil. The name oxykinoshitalite was assigned as dictated by the IMA-approved nomenclature of the mica-group minerals (Rieder *et al.* 1998). The species and name have been approved by the International Mineralogical Association Commission on New Minerals and Mineral Names (IMA 2004–013). Holotype material is deposited at the Canadian Museum of Nature, Ottawa, Canada.

OCCURRENCE AND MINERAL ASSOCIATION

Oxykinoshitalite was found in olivine nephelinite on Fernando de Noronha Island, Pernambuco, Brazil. The principal minerals of the nephelinite are olivine, clinopyroxene, Fe–Ti oxide and nepheline; accessory minerals are calcite, apatite, K-feldspar and kinoshitalite. Oxykinoshitalite is bright orange to brownish and occurs as small irregularly shaped interstitial crystals 0.03–0.05 mm in diameter. Almeida (1955) distinguished three periods of volcanic activity on Fernando de Noronha Island and three corresponding formations: (1) the Remedios Formation, (2) the Quixaba Formation, and (3) the Sao Jose Formation. Olivine nephelinite containing oxykinoshitalite belongs to the Quixaba Formation, which is dominated by nepheline basalt flows with minor nephelinite dykes, tuffs and breccias.

TABLE 1. CHEMICAL COMPOSITION (wt.%) AND UNIT FORMULAE (*apfu*) OF MINERALS FROM OLIVINE NEPHELINITE, FERNANDO DO NORONHA

	Clinopyroxene	Fe-Ti oxide	Nepheline	Olivine	Calcite
SiO_2	46.31	0.61	42.45	38.97	0.24
TiO_2	3.28	21.81	0.10	0.03	0.01
Al_2O_3	5.17	0.80	34.24	0.06	0.11
Cr_2O_3	0.02	0.26	0.01	0.03	0.15
FeO	8.23	63.41	1.17	14.13	0.11
MnO	0.02	0.58	0.02	0.23	0.09
MgO	12.60	4.13	0.17	44.93	0.36
CaO	22.68	0.20	0.96	0.03	57.18
NiO	0.01	0.05	0.01	0.14	0.00
Na_2O	0.60	0.05	13.82	0.03	0.07
K_2O	0.02	0.01	5.53	0.01	0.04
P_2O_5	0.19	0.03	0.02	0.02	0.02
CO_2	–	–	–	–	41.16
Total	99.13	91.94	98.69	98.61	99.54
Si	1.76	0.03	1.02	0.99	0.00
Ti	0.09	0.69	0.00	0.00	0.00
Al	0.23	0.04	0.98	0.00	0.00
Cr	0.00	0.01	0.00	0.00	0.00
Fe	0.26	2.22	0.02	0.30	0.00
Mn	0.00	0.02	0.00	0.01	0.00
Mg	0.71	0.26	0.01	1.70	0.01
Ca	0.92	0.01	0.03	0.00	1.02
Ni	0.00	0.00	0.00	0.00	0.00
Na	0.04	0.00	0.65	0.00	0.00
K	0.00	0.00	0.17	0.00	0.00
P	0.01	0.00	0.00	0.00	0.00
C	–	–	–	–	0.96
catsum	4.02	3.27	2.88	3.00	1.99
anion basis	O = 6	O = 4	O = 4	O = 4	O = 3

PHYSICAL AND OPTICAL PROPERTIES

Oxykinoshitalite varies from bright orange to brown with a brown streak. It is brittle, $H = 2.5$, $D_{obs} = 3.3(1)$, $D_{calc} = 3.45$ g/cm^3, has a vitreous luster and does not fluoresce in ultraviolet light. It has perfect cleavage on {001} (Fig. 1) and a splintery fracture. A spindle stage was used to orient a crystal for measurement of indices of refraction and determination of $2V$ with extinction curves. The optic orientation was determined by transferring the crystal from the spindle stage to a precession camera and determining the relative axial relations by X-ray diffraction. In transmitted plane-polarized light, oxykinoshitalite is strongly pleochroic, with X pale brown, $Y \approx Z$ deep red-brown; $X \wedge c = 2°$ (in β obtuse), $Y = b$, $Z \wedge a = 8°$ (in β obtuse) with absorption $X < Y \approx Z$. It is biaxial positive, α 1.708 ± 0.001, β 1.710 ± 0.001, γ 1.719 ± 0.001, $2V_{obs}$ 56 ± 2°, $2V_{calc}$ 51°.

CHEMICAL COMPOSITION

The chemical composition was determined for 25 crystals of oxykinoshitalite, together with several of the coexisting minerals, with a Cameca SX 100 electron microprobe operating in wavelength-dispersion mode with an accelerating voltage of 15 kV, a beam current of 20 nA, a beam size of 20 μm and counting times on peak and background of 20 and 10 s, respectively. The following standards and crystals were used for K or L X-ray lines: F, zinnwaldite; Mg, forsterite; Al, Na, jadeite; Ca, diopside; Si, K, sanidine; Cl, tugtupite; Ti, titanite; Cr, chromite; Mn, spessartine; Fe, fayalite; Ni, pentlandite; Ba, barite. Data were reduced using the $\phi(\rho z)$ procedure (Merlet 1992). Chemical compositions and empirical formulae of the coexisting minerals are given in Table 1. Chemical compositions for oxykinoshitalite were determined on single grains extracted from the rock. There was the usual problem of charging associated with analyzing very small grains, and totals are somewhat low (by 2–3 wt.%) for most grains. However, compositions are fairly uniform, and the few we were able to obtain on larger grains do have good analytical totals (Table 2). The composition and unit formula of the crystal chosen for crystal-structure determination are also given in Table 2.

Ion-microprobe analysis was done on a Cameca IMS 4f. Owing to the very small dimensions of the mica crystal, an $^{16}O^-$ primary beam <5 μm in diameter, corresponding to a beam current of ~1.5–2 nA, was used. Analytical methods for H, Li and B were similar to those described by Ottolini *et al.* (2002). The sample

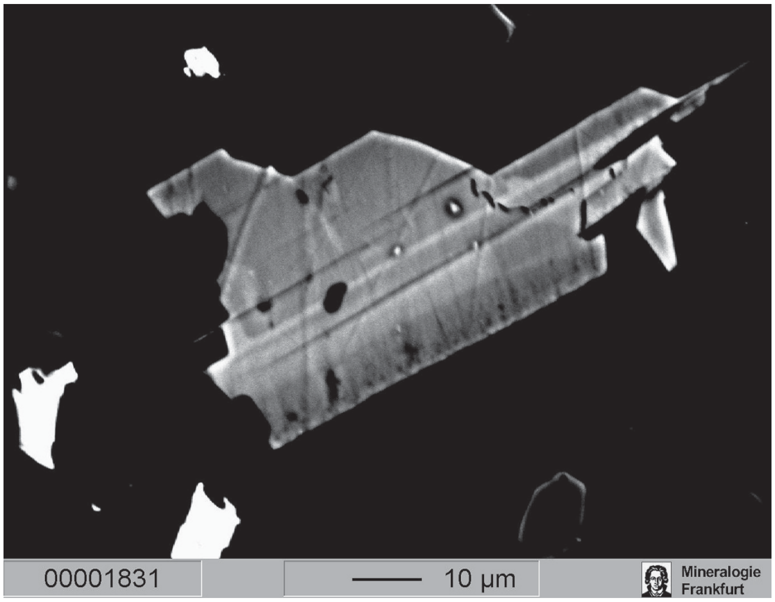

FIG. 1. Back-scattered-electron image of oxykinoshitalite, showing the prominent (001) cleavage.

TABLE 2. CHEMICAL COMPOSITION (wt.%) AND UNIT FORMULA* (*apfu*) OF OXYKINOSHITALITE

	Large crystal	X-ray crystal **		Large crystal	X-ray crystal
SiO_2	28.92	26.96	Si	2.46	2.36
TiO_2	11.94	11.63	Al	1.53	1.60
Al_2O_3	15.26	15.48	Fe^{3+}	0.01	0.04
$Fe_2O_3^*$	0.00	0.90	ΣT	4.00	4.00
FeO	12.00	11.37			
MnO	0.14	0.12	Ti	0.76	0.77
MgO	10.74	10.58	Fe^{3+}	0.00	0.02
BaO	15.49	13.91	Fe^{2+}	0.85	0.83
CaO	0.03	0.15	Mg	1.36	1.38
K_2O	4.05	3.84	Mn	0.01	0.01
Na_2O	0.39	0.41	Σ	2.98	3.01
H_2O	0.55	0.55			
F	0.91	0.92	Ba	0.52	0.48
Cl	–	0.06	Ca	–	0.01
O=F	–0.38	–0.39	K	0.44	0.43
O=Cl	–	–0.01	Na	0.06	0.07
			Σ	1.02	0.99
Σ	100.04	96.49			
			F	0.24	0.26
			OH	0.31	0.32
			O^{2-}	1.45	1.42

* Calculated on the basis of 12 (O + OH + F) *apfu*, with Fe^{3+} calculated for electroneutrality. ** Includes 0.017and 0.0021 wt.% Li and B, respectively.

TABLE 3. X-RAY POWDER-DIFFRACTION DATA FOR OXYKINOSHITALITE

I	d_{meas} (Å)	d_{calc} (Å)	*h k l*	I	d_{meas} (Å)	d_{calc} (Å)	*h k l*
1	4.932	4.947	0 0 2	**9**	2.172	2.169	$\bar{1}$ 3 3
2	4.157	4.198	0 2 1	5	1.988	1.989	1 3 3
2	3.941	3.934	1 1 1	5	1.661	1.661	$\bar{1}$ 3 5
7	3.646	3.649	$\bar{1}$ 1 2	3	1.627	1.633	$\bar{1}$ 1 6
6	3.383	3.383	0 0 2	3	1.592	1.585	2 4 2
7	3.130	3.131	1 1 2	5	1.547	1.548	3 1 2
5	2.902	2.893	$\bar{1}$ 1 3	5	1.526	1.523	$\bar{2}$ 0 6
10	2.637	2.633	$\bar{1}$ 3 1	4	1.351	1.350	1 3 6
5	2.435	2.441	2 0 1	4	1.331	1.333	2 6 0
				4	1.311	1.311	0 6 4

Refined cell: *a* 5.350(11), *b* 9.273(13), *c* 10.049(12) Å, β 100.084(14)°, *V* 490.8(9) Å^3.

was left in the ion-microprobe sample chamber to degas for two days, together with H standards that were used in the calibration procedure. The energy-filtering technique was used to eliminate any possible molecular interference and to reduce matrix effects affecting light-element ionization. Secondary positive-ion currents were measured at masses 1 (H), 7 (Li) and 30 (Si was used as the reference element), and corrected for isotopic abundances. The results were put on a quantitative basis using empirical calibration curves based on standard silicate samples. In particular, for H quantification we used the extrapolated regression line: IY(H/Si) *versus* (Fetot + Mn + Ti), derived for kornerupine (Ottolini & Hawthorne 2001) and tested successfully with tourmaline standards, to take into account any variation in IY(H/Si) in the oxy-mica (which could not have a significant effect owing to the high amount of (Fetot + Mn + Ti) in this sample.

The quantification of Li and B concentration was done according to the procedure of Ottolini *et al.* (1993). The accuracy of H and Li results is estimated to be in the order of 10% relative.

X-RAY POWDER DIFFRACTION

The powder-diffraction pattern was recorded with Ni-filtered Cu$K\alpha$ X-radiation (λ = 1.54178 Å) and a 114.6 mm Gandolfi camera. Table 3 shows the X-ray powder-diffraction data for oxykinoshitalite, together with the refined cell-dimensions; these values are in reasonable accord with those determined by single-crystal diffractometry.

X-RAY DATA COLLECTION AND STRUCTURE REFINEMENT

X-ray single-crystal diffraction data for oxykinoshitalite were collected with a Bruker *P*4 diffractometer equipped with a CCD detector (Mo$K\alpha$ radiation) from a thin plate with dimensions 0.004 × 0.05 × 0.05 mm. The intensities of 4237 reflections with $\bar{7} < h < 7$, $\overline{12} < k < 11$, $\overline{14} < l < 14$ were collected to 59.8°2θ using 30 s per 0.15° frame: an empirical absorption-correction (SADABS, Sheldrick 1998) was applied. The refined unit-cell parameters were obtained from 1632 reflections with $I > 10\sigma I$ (Table 4) and indicate that this crystal has the 1*M* polytype structure. On a basis of 585 unique ($F_o > 4\sigma F$) reflections, the crystal structure was refined to R_1 = 4.27% and a Go*F* value of 1.052 with the SHELXTL package of programs (Sheldrick 1997). Details of the data collection and structure refinement are given in Table 4, final atom parameters are given in Table 5, selected interatomic distances and angles in Table 6, refined site-scattering values in Table 7, and bond valences in Table 8. A table of structure factors may be obtained from the Depository of Unpublished Data, CISTI, National Research Council, Ottawa, Ontario K1A 0S2, Canada.

DISCUSSION

Unit formula

A critical issue with regard to the unit formula of oxykinoshitalite is the oxidation state of Fe. As only a few tiny grains were available for study, it was not feasible to determine the Fe^{2+} and Fe^{3+} contents spectroscopically. However, for oxykinoshitalite, we have measured the abundance of *all* other cation components of the mineral (including H), and hence we may calculate the amount of Fe^{3+} (note that this situation is very different from the usual case, where only electron-microprobe data are available and the content of H has not been measured). The Fe^{3+} content was so calculated for analysis (2) of Table 2; a value of 0.06 Fe^{3+} *apfu* was obtained, similar to the deficiency in Si + Al at the *T* site: 0.03 *pfu*. This accord suggests that a small amount of Fe^{3+} occurs at the *T* site, and Fe^{2+} occurs at the *M* sites.

Site populations

In the crystal structure of oxykinoshitalite, there is one *T* site with ($Si_{2.38}$ $Al_{1.62}$) *apfu* (normalized to full occupancy) and <*T*–O> = 1.671 Å. Figure 2 shows the variation in <*T*–O> as a function of Al content for trioctahedral and dioctahedral micas (data from Mottana *et al.* 2002) and oxykinoshitalite. We excluded synthetic micas and micas with major Si, Fe^{3+}, Mn and Ti at the *T* site. The regression line was calculated omitting data in the right upper corner of the diagram, a group of brittle micas from skarns and marbles with very high Al at the *T* site. Oxykinoshitalite lies on this line, indicating that the <*T*–O> distance is in accord with the assigned site-population.

TABLE 4. MISCELLANEOUS REFINEMENT DATA FOR OXYKINOSHITALITE

a (Å)	5.3516(7)	Crystal size (mm)	0.004 × 0.05 × 0.05
b	9.2817(11)		
c	10.0475(13)	Radiation/filter	Mo$K\alpha$/graphite
β (°)	100.337(3)	2θ range for data collection (°)	59.93
V (Å^3)	490.98(18)	*R*(int) (%)	4.8
Space group	*C*2/*m*	Reflections collected	4237
		Independent reflections	762
		$F_o > 4\sigma F$	585
Z	2	Refinement method	Full-matrix least squares on F^2, fixed weights ∝ $1/\sigma\,|F_o^2|$
Absorption coefficient (mm^{-1})	4.57	Goodness of fit on F^2	1.052
F(000)	483.3	Final $R_{(obs)}$ (%) [$F_o > 4\sigma F$]	R_1 = 4.27
D_{calc} (g/cm^3)	3.450	*R* indices (all data) (%)	R_1 = 6.29 wR_2 = 9.85 Go*F* = 1.052

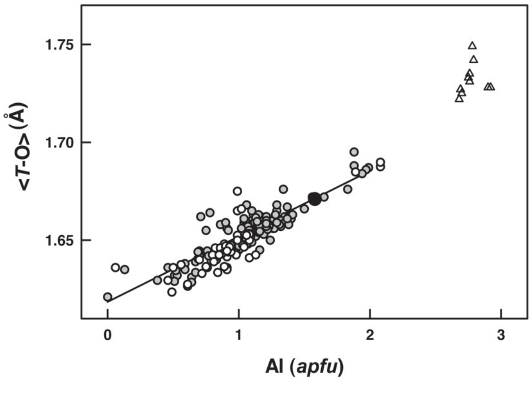

FIG. 2. Content of Al (*apfu*) as a function of <*T*–O> distance in micas. Empty small circles: trioctahedral micas, triangles: trioctahedral brittle micas from skarns and marbles with very high Al content at the *T* site, small gray circles: dioctahedral micas; large black circle: oxykinoshitalite (this paper).

TABLE 5. FINAL ATOM POSITIONS AND DISPLACEMENT PARAMETERS FOR OXYKINOSHITALITE

	x	y	z	U_{11}	U_{22}	U_{33}	U_{23}	U_{13}	U_{12}	Ueq
I	0	0	0	0.0197(5)	0.0205(5)	0.0285(5)	0	0.0046(4)	0	0.0229(3)
T	0.5736(2)	0.16750(11)	0.22032(11)	0.0083(5)	0.0106(5)	0.0145(6)	0.0001(4)	0.0024(4)	–0.0005(4)	0.0111(3)
M(1)	0	1/2	1/2	0.0082(8)	0.0065(8)	0.0167(9)	0	0.0043(6)	0	0.0102(5)
M(2)	0	0.15509(12)	1/2	0.0067(6)	0.0175(7)	0.0139(6)	0	0.0014(4)	0	0.0127(4)
O(1)	0.8179(6)	0.2354(3)	0.1586(3)	0.0192(16)	0.0287(16)	0.0210(17)	–0.0030(13)	0.0060(12)	–0.0075(13)	0.0227(7)
O(2)	0.6314(5)	0.1709(3)	0.3903(3)	0.0120(13)	0.0107(13)	0.0180(15)	0.0007(10)	0.0031(11)	–0.0007(10)	0.0135(6)
O(3)	0.5223(8)	0	0.1603(4)	0.029(2)	0.0163(19)	0.013(2)	0	–0.0012(17)	0	0.0202(9)
O(4)	0.1257(7)	0	0.3964(4)	0.0093(18)	0.023(2)	0.016(2)	0	0.0031(15)	0	0.0160(8)

TABLE 6. SELECTED INTERATOMIC DISTANCES (Å) AND ANGLES (°) FOR OXYKINOSHITALITE

T–O(1)		1.668(3)	M(1)–O(2)	×4	2.122(3)
T–O(1)a		1.663(3)	M(1)–O(4)	×2	2.085(4)
T–O(2)		1.680(3)	<M(1)–O>		2.110
T–O(3)		1.672(2)			
<T–O>		1.671	I–O (inner)		
			I–O(3)	×2	2.965(4)
M(2)–O(2)b	×2	2.085(3)	I–O(1)	×4	2.970(3)
M(2)–O(2)c	×2	2.144(3)	<I–O>$_{\text{(inner)}}$		2.968
M(2)–O(4)	×2	1.965(3)			
<M(2)–O>		2.065	I–O (outer)		
			I–O(1)	×4	3.239(3)
			I–O(3)	×2	3.257(4)
			<I–O>$_{\text{(outer)}}$		3.245

a: $x - ½, -y + ½, z$; b: $x - 1, y, z$; c: $-x + ½, -y + ½, -z + 1$.

TABLE 7. REFINED SITE-SCATTERING VALUES (*epfu*) AND ASSIGNED SITE-POPULATIONS (*apfu*) FOR OXYKINOSHITALITE

	Refined site-scattering	Site population	Calculated site-scattering	$(M\text{–}\varphi)_{\text{calc}}$* (Å)	$(M\text{–}\varphi)_{\text{obs}}$ (Å)
T	–	2.36 Si + 1.60 Al + 0.04 Fe^{3+}	56.0	–	–
M(1)	17.8(1)	0.53 Mg + 0.40 Fe^{2+} + 0.07 Ti^{4+}	18.3	2.106	2.110
M(2)	36.5(2)	0.84 Mg + 0.70 Ti^{4+} + 0.46 Fe^{2+}	37.4	2.063	2.065

* Radii from Shannon (1976).

TABLE 8. BOND-VALENCE* TABLE FOR OXYKINOSHITALITE

	T	M(1)	M(2)	I	Σ
O(1)	0.91 0.92			$0.12^{\times4}\downarrow$ $0.06^{\times4}\downarrow$	2.01
O(2)	0.88	$0.35^{\times4}\downarrow$	$0.40^{\times2}\downarrow$ $0.35^{\times2}\downarrow$		1.98
O(3)	$0.90^{\times2}\rightarrow$			$0.12^{\times2}\downarrow$ $0.06^{\times2}\downarrow$	1.98
O(4)		$0.40^{\times2}\downarrow$	$0.57^{\times2}\downarrow\rightarrow$		1.54
Σ	3.61	2.20	2.64	1.08	

* The bond valences (*vu*) for Ba, Sr and K from the curves of Brown & Altermatt (1985); for Ti, Fe^{2+}, Mg and Mn^{2+}, we used the parameters of Brown (1981).

There are two octahedrally coordinated sites, M(1) and M(2), that are occupied by the M-type cations of the formula unit (Table 2). The cations were initially assigned to each site on the basis of the refined site-scattering values, together with the observation that the <M(2)–O> distance (2.065 Å) is significantly less than the <M(1)–O> distance (2.110 Å) and hence the majority of the smallest cation (Ti^{4+}) must occur at the M(2) site. The sum of the refined site-scattering values at the M sites is 54.3 *epfu* (electrons per formula unit), close to the analogous value calculated from the unit formula of Table 2: 55.7 *epfu*. We will reduce this value to 55.4 *epfu* to correspond with an M-cation sum of 3.0 *apfu*. In order to assign the cations, we will modify the refined site-scattering values by the factor 55.4 / 54.3 such that the refined values are exactly in accord with the unit formula. Initially, all Ti was assigned to M(2), and the Mg and Fe (including 0.01 Mn^{2+}) populations were calculated from the modified site-scattering values, resulting in the following site-populations: M(1): 0.53 Mg + 0.40 Fe^{2+} + 0.07 Ti^{4+}; M(2): 0.84 Mg + 0.70 Ti^{4+} + 0.46 Fe^{2+}. We may now compare the observed mean bond-lengths with the values calculated from the constituent empirical ionic radii. The mean anion radius for each site is the same: $(1.42 \times 1.36 + 0.32 \times 1.34 + 0.26 \times 1.30 + 1.38 \times 2.00) / 2 = 1.370$ Å. Summing this anion radius and the constituent-cation radius for each site gives the following calculated (observed) values: <M(1)–O> = 2.119 (2.110); <M(1)–O> = 2.057 (2.065) Å. We may adjust the amount of Ti^{4+} at each site while keeping the calculated scattering-values constant to arrive at the best fit for the observed and calculated distances (*i.e.*, an equally good fit at each site). This procedure results in the site populations given in Table 7.

Short-range order around the O(4) site

The O(4) site is occupied by both O^{2-} and $(OH,F)^-$, and is surrounded by one *M*(1) site and two *M*(2) sites (Fig. 3, Table 8). According to the arguments of Hawthorne (1997), the short-range arrangements around the O(4) site should lead to local satisfaction of the valence-sum rule of Brown (1981). Where O(4) is occupied by $(OH)^-$ or F^-, the sum of the bond valences incident at O(4) should be equal to 1 *vu* (valence unit); in kinoshitalite, the *M*(1) and *M*(2) sites are occupied by Mg or Fe^{2+}, and hence the bond valence incident at O(4) is 2/6 per *M* site, which is $1/3 \times 3 = 1$ *vu*, in accord with the valence-sum rule. Where O(4) is occupied by O^{2-}, the sum of the bond valences incident at O(4) should be equal to 2 *vu*. It is less straightforward to estimate the bond valences in this case, as we know from the structure (Fig. 3) that the *M*(2) sites are closer to O(4) than in a normal (OH)-rich mica, and we do not know the *local* Ti^{4+}–O, Fe^{2+}–O and Mg–O distances. However, we may estimate the distances in the following way and see if they are realistic. The Pauling bond-strengths for the Ti^{4+}–O, Fe^{2+}–O and Mg–O bonds are 0.67, 0.33 and 0.33 *vu*, respectively, with a sum of 1.34 *vu*. Increasing each value by 50% gives 1.00, 0.50 and 0.50 *vu*, with a sum of 2.00 *vu*. The analogous distances are as follows: 1.789, 2.006 and 1.906 Å, respectively, which are short but reasonable distances for these cations. Thus we expect a local coordination of $(Mg,Fe^{2+})_2Ti^{4+}$ around O^{2-} at O(4). The composition of the O(4) site in oxykinoshitalite is $\{O^{2-}_{1.44}\ (OH,F)_{0.56}\}$. Given the local coordinations around the different anions at O(4), we expect the following content of the *M* sites: $\{(Mg,Fe^{2+})_2Ti^{4+}\}_{1.42/2}$ [coordinating $O^{2-}_{1.44}$] and $\{(Mg,Fe^{2+})MgMg\}_{0.58/2}$ [coordinating $(OH,F)_{0.58}$]. The sum of these values, $(Mg + Fe^{2+})_{2.29}Ti_{0.71}$, thus is in quite reasonable agreement with the unit formula determined from electron-microprobe analysis: $(Mg + Fe^{2+} + Mn^{2+})_{2.23}\ Ti^{4+}_{0.77}$, indicating that our arguments for the local configurations around the O(4) site are reasonable.

Layer adjustment

There are two polytypes of kinoshitalite, 1*M* and $2M_1$ (Yoshii *et al.* 1973a), and the 1*M* polytype is more common. Calculated structural parameters for the structure refined here are given in Table 9. The tetrahedron-rotation angle, α, the rotation of adjacent tetrahedra in opposite directions in the (001) plane, is a measure of the misfit between the sheets of octahedra and tetrahedra. In oxykinoshitalite, the tetrahedron-rotation angle is rather small (α = 5.92°). Guggenheim & Frimmel (1999) showed that there is a correlation between α and amount of Fe^{2+} at the *M* sites: the relatively large size of Fe in the octahedra allows a better fit to the small tetrahedron-rotation angle. Less rotation of the tetrahedra implies a larger silicate ring, which allows Ba to fit within the ring, accounting for the rather small interlayer separation in oxykinoshitalite (3.221 Å).

TABLE 9. CALCULATED STRUCTURAL PARAMETERS FOR OXYKINOSHITALITE

τ (°)*	111.25	Δz_{ave} (Å)†	0.017
α (°)**	5.92	Sheet thickness $_T$ (Å)	2.327
$\psi_{M(1)}$ (°)***	58.49	Sheet thickness $_O$ (Å)	2.206
$\psi_{M(2)}$ (°)***	57.72	Interlayer separation$_I$ (Å)	3.221

* τ = mean O_b–*T*–O_a angle
** tetrahedron rotation angle $\alpha = \Sigma^6{}_{i=1}\ \alpha_i/6$, $\alpha_i = |120 - \varphi_i|$, where φ_i is the angle between basal edges of neighboring tetrahedra in the ring
*** $\psi = \cos^{-1}$ [octahedron thickness / 2 (*M*–O,OH,F)]
† corrugation of plane of basal oxygen atoms $\Delta z_{ave} = (zO_{basal(max)} - zO_{basal(min)}) \times c \sin\beta$

In the crystal structure of oxykinoshitalite, the O(4) site is occupied by $(O_{1.44}\ OH_{0.31}\ F_{0.24})$ and O^{2-} is dominant at this site. Ohta *et al.* (1982) suggested that the lack of H atoms decreases both the interlayer separation and the *c* parameter. For our structure, the interlayer thickness is rather small: 3.221 Å. The *c* cell parameter [10.0475(13) Å] is smaller than those reported for OH-dominant kinoshitalite [Kato *et al.* (1979): 10.256(8) Å,

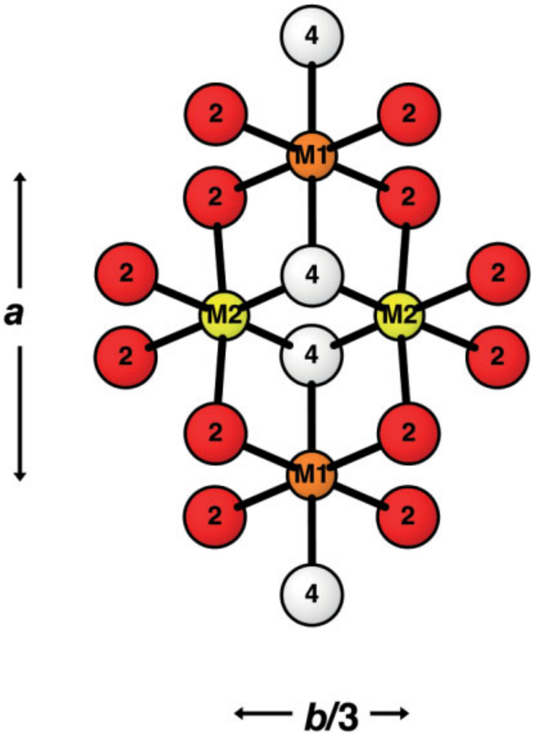

FIG. 3. The *M*(1) and *M*(2) sites and their coordinations in oxykinoshitalite. *M*(1): orange circles, *M*(2): yellow circles, O(2): numbered brown circles, and O(4): numbered white circles.

Gnos & Ambruster (2000): 10.197(2) Å, Guggenheim & Frimmel (1999): 10.054(2) Å].

Cation–anion substitutions

In the crystal investigated, there are four types of cation substitution and one type of anion substitution: (1) K ↔ Ba substitution at the interlayer site, (2) Si ↔ (Al,Fe^{3+}) substitution at the *T* site, (3) (Mg,Fe^{2+}) ↔ Ti^{4+} substitution at the *M* sites [primarily at the *M*(2) site], (4) (Mg,Fe^{2+}) ↔ Fe^{3+} at the *M* sites, and (5) O ↔ (OH,F) substitution at the O(4) site.

Yoshii *et al*. (1973b), Greenwood (1998) and Ibhi & Nachit (2000) indicated that the major exchange-reaction relating Ba-poor micas and Ba-rich micas is Ba + Al ↔ K + Si (which we will designate as substitution [1]). The data of Kato *et al*. (1979), Solie & Su (1987), Dasgupta *et al*. (1989), Guggenheim & Frimmel (1999), Gnos & Ambruster (2000) and the present study are in accord with this reaction (Fig. 4), thus coupling substitutions (1) and (2) listed above.

By analogy with the amphiboles (Oberti *et al*. 1992, Hawthorne *et al*. 1998), we expect Ti^{4+} to enter the sheet of octahedra in micas *via* $M^{2+} + (OH)_2 \leftrightarrow Ti^{4+} + O^{2-}_2$ (designated as substitution [2] above). The composition of oxykinoshitalite, with 0.75 Ti^{4+} and 1.44 O^{2-}, is almost exactly in accord with this substitution.

Site preference for Ti^{4+}

The assigned site-populations indicate that Ti^{4+} is very strongly ordered at the *M*(2) site. The local environment is shown in Figure 3; note that this fragment of the mica structure is very similar to the analogous fragment in the structure of a monoclinic amphibole. In Figure 3, the O(4) site is occupied by (OH)$^-$, F$^-$ and O^{2-}. Where an O(4) site is locally occupied by a monovalent anion, the local (short-range) coordination is MgMgMg at *M*(1)*M*(2)*M*(2), the incident bond-valence at O(4) is approximately equal to 1 *vu*, and the valence-sum rule (Brown 1981) is satisfied at short range (Hawthorne 1997). Where an O(4) site is locally occupied by a divalent anion, the local (short-range) coordination must provide an incident bond-valence at O(4) of approximately equal to 2 *vu*. This requires occupancy of one or more of the locally associated *M* sites by a higher-valence cation (*i.e*., Ti^{4+} in this case). If Ti^{4+} is incorporated into the mica structure by the substitution $M^{2+} + (OH)^-_2 \leftrightarrow Ti^{4+} + O^{2-}_2$, occurrence of Ti^{4+} at the *M*(2) site means that Ti^{4+} can move toward two O(4) sites, as the two O(4) sites around the *M*(2) site are in the *trans* configuration. If Ti^{4+} were incorporated at the *M*(1) site, Ti^{4+} could move only toward one O(4) site and away from another O(4) site, as the two O(4) sites around the *M*(1) site are in the *cis* configuration. This stereochemical argument provides us with a simple reason for the observed site-preference of Ti^{4+} in oxykinoshitalite.

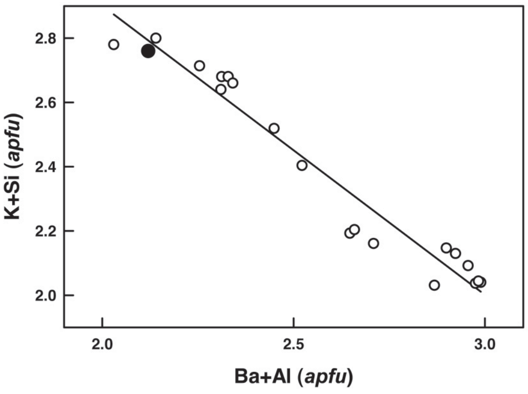

FIG. 4. Content of K + Si (*apfu*) as a function of Ba + Al (*apfu*) in various samples of kinoshitalite (open circles), from the data from Guggenheim & Frimmel (1999), Solie & Su (1987), Kato *et al*. (1979), Gnos & Ambruster (2000) and Dasgupta *et al*. (1989). In the black circle, we show the data for oxykinoshitalite.

End-member formula

The issue of an end-member formula is rather ambiguous in the case of oxykinoshitalite. Normally, we may write the end-member formula by filling each site by the dominant cation or anion at that site, within the constraints of electroneutrality. Inspection of Table 2 shows that Ba is dominant at the *I* site, Mg is dominant at the *M*(1) and *M*(2) sites (see also Table 7), Si is dominant at the *T* site, and O is dominant at the O(4) site. The resultant formula is thus $Ba\ Mg_3\ Si_4\ O_{10}\ O_2$. This formula bears little resemblance to the empirical formula of the mineral. Moreover, the formula $Ba\ Mg_3\ Si_4\ O_{10}\ O_2$ cannot be stable, as the O^{2-} anion at O(4) would be coordinated by three Mg^{2+} cations; this arrangement would violate the valence-matching principle and hence cannot occur. As discussed above, O^{2-} will be incorporated into the structure *via* the substitution $M^{2+} + (OH)_2 \leftrightarrow Ti^{4+} + O^{2-}_2$, which indicates that Ti^{4+} is an essential constituent. Taking the end-member formula of kinoshitalite as $Ba\ Mg_3\ (Si_2\ Al_2)\ O_{10}\ (OH)_2$, replacement of $(OH)_2$ by O^{2-}_2 according to the above substitution leads to the formula $Ba\ (Mg_2\ Ti^{4+})\ (Si_2\ Al_2)\ O_{10}\ O_2$. In this composition, O^{2-} will then be coordinated by $Mg_2\ Ti^{4+}$, which is more in accord with the valence-sum rule (Brown 1981). The formula $Ba\ (Mg_2\ Ti^{4+})\ (Si_2\ Al_2)\ O_{10}\ O_2$ is not an end-member as it does not accord with necessary criteria (Hawthorne 2002). However, this is a common situation with micas (and other complex rock-forming minerals), and the pragmatic situation may be to consider $Ba\ (Mg_2Ti^{4+})\ (Si_2Al_2)\ O_{10}\ O_2$ as the ideal composition of oxykinoshitalite.

SUMMARY

(1) The oxykinoshitalite investigated here occurs in olivine nephelinite with a high content of Ba, Ti^{4+} and Fe.

(2) Our sample has very high contents of Ti (0.76 *apfu*) and Fe^{3+} (0.57 *apfu*) and very low content of Mn^{2+}.

(3) There are two main exchange-reactions in oxykinoshitalite: (i) $^{I}K + {}^{T}Si \leftrightarrow {}^{I}Ba + {}^{T}Al$, and (ii) $^{M}Mg + {}^{A}(OH)_2 \leftrightarrow {}^{M}Ti^{4+} + {}^{A}O^{2-}{}_2$.

(4) The dominance of O atoms at the O(4) site indicates that oxykinoshitalite from Fernando de Noronha Island, Brazil, is a new mineral species.

ACKNOWLEDGEMENTS

FCH was supported by a Canada Research Chair in Crystallography and Mineralogy and by Major Facilities Access, Equipment and Discovery Grants from the Natural Sciences and Engineering Research Council of Canada. YAU is supported by a University of Manitoba Graduate Fellowship and Manitoba Graduate Scholarship.

REFERENCES

Almeida, F.F.M. (1955): Geologia e petrologia do arquipelago de Fernando de Noronha. *Div. Geol. Mineral., Dep. Prod. Mineral, Rio de Janeiro, Monogr.* **13**.

Ankinovich, S.G., Ankinovich, Ye.A., Rozdestvenskaya, I.V. & Frank-Kamenetsky, V.A. (1973): Chernykhite, a new barium – vanadium mica from northwestern Karatau. *Int. Geol. Rev.* **15**, 641-647.

Brigatti, M.F. & Poppi, L. (1993): Crystal chemistry of Ba-rich trioctahedral mica-1M. *Eur. J. Mineral.* **5**, 857-871.

Brown, I.D. (1981): The bond-valence method: an empirical approach to chemical structure and bonding. *In* Structure and Bonding in Crystals II (M. O'Keeffe & A. Navrotsky, eds.). Academic Press, New York, N.Y. (1–30).

________ & Altermatt, D. (1985): Bond-valence parameters obtained from a systematic analysis of the inorganic crystal structure database. *Acta Crystallogr.* **B41**, 244-247.

Dasgupta, S., Chakraborti, S., Sengupta, P., Bhattacharya, P.K., Banerjee, H. & Fukuoka, M. (1989): Compositional characteristics of kinoshitalite from the Sausar Group, India. *Am. Mineral.* **74**, 200-202.

Gaspar, J.C. & Wyllie, P.J. (1982): Barium phlogopite from the Jacupiranga carbonanite, Brazil. *Am. Mineral.* **67**, 997-1000.

Gnos, E. & Armbruster, T. (2000): Kinoshitalite, $Ba(Mg)_3(Al_2Si_2)O_{10}(OH,F)$, a brittle mica from a manganese deposit in Oman: paragenesis and crystal chemistry. *Am. Mineral.* **85**, 242-250.

Graeser, S., Hetherington, C.J. & Gieré, R. (2003): Ganterite, a new barium-dominant analogue of muscovite from the Berisal complex, Simplon region, Switzerland. *Can. Mineral.* **41**, 1271-1280.

Greenwood, J.C. (1998): Barian–titanian micas from Ilha da Trindade, South Atlantic. *Mineral. Mag.* **62**, 687-695.

Guggenheim, S. & Frimmel, H.E. (1999): Ferrokinoshitalite, a new species of brittle mica from the Broken Hill mine, South Africa: structural and mineralogical characterization. *Can. Mineral.* **37**, 1445-1452.

________ & Kato, T. (1984): Kinoshitalite and Mn phlogopites: trial refinements in subgroup symmetry and further refinement in ideal symmetry. *Mineral. J.* **12**, 1-5.

Hawthorne, F.C. (1997): Short-range order in amphiboles: a bond-valence approach. *Can. Mineral.* **35**, 203-218.

________ (2002): The use of end-member charge-arrangements in defining new mineral species and heterovalent substitutions in complex minerals. *Can. Mineral.* **40**, 699-710.

________, Oberti, R., Zanetti, A. & Czamanske, G.K. (1998): The role of Ti in hydrogen-deficient amphiboles: sodic–calcic and sodic amphiboles from Coyote Peak, California. *Can. Mineral.* **36**, 1253-1265.

Hetherington, C.J., Gieré, R. & Graeser, S. (2003): Composition of barium-rich white micas from the Berisal complex, Simplon region, Switzerland. *Can. Mineral.* **41**, 1281-1291.

Ibhi, A. & Nachit, H. (2000): The substitution mechanism of Ba and Ti into phyllosilicate phases: the example of barium–titanitum biotite. *Ann. Chim. Sci. Mat.* **25**, 627-634.

Kato, T., Miúra, Ya., Yoshii, M. & Maeda, K. (1979): The crystal structures of 1*M*-kinoshitalite, a new barium brittle mica and 1*M*-manganese trioctahedral micas. *Mineral. J.* **9**, 392-408.

Mansker, W.L., Ewing, R.C. & Keil, K. (1979): Barian–titanian biotites in nephelinites from Oahu, Hawaii. *Am. Mineral.* **64**, 156-159.

McCauley, J.W. & Newnham, R.E. (1973): Structure refinement of a barium mica. *Z. Kristallogr.* **137**, 360-367.

________, ________ & Gibbs, G.V. (1973): Crystal structure analysis of synthetic fluorophlogopite. *Am. Mineral.* **58**, 249-254.

Merlet, C. (1992): Quantitative electron probe microanalysis: new accurate $\phi(\rho z)$ description. *Mikrochim. Acta* **12**, 107-115.

Mottana, A., Sassi, F.P., Thompson, J.B., Jr. & Guggenheim, S., eds. (2002): Micas: Crystal Chemistry and Metamorphic Petrology. *Rev. Mineral. Geochem.* **46**.

OBERTI, R., UNGARETTI, L., CANNILLO, E. & HAWTHORNE, F.C. (1992): The behaviour of Ti in amphiboles. I. Four- and six-coordinate Ti in richterite. *Eur. J. Mineral.* **4**, 425-439.

OHTA, T., TAKEDA, H. & TAKÉUCHI, Y. (1982): Mica polytypism: similarities in the crystal structures of coexisting $1M$ and $2M_1$ oxybiotites. *Am. Mineral.* **67**, 298-310.

OTTOLINI, L., BOTTAZZI, P. & VANUCCI, R. (1993): Quantification of Li, Be and B in silicates by secondary ion mass spectrometry using conventional energy filtering. *Anal. Chem.* **65**, 1960-1968.

________, CÁMARA, F., HAWTHORNE, F.C. & STIRLING, J. (2002): SIMS matrix effects in the analysis of light elements in silicate minerals: comparison with SREF and EMPA data. Am. *Mineral.* **87**, 1477-1485.

________ & HAWTHORNE, F.C. (2001): SIMS ionization of hydrogen in silicates: a case study of kornerupine. *J. Anal. At. Spectr.* **16**, 1266-1270.

PATTIARATCHI, D.B., SAARI, E. & SAHAMA, T.G. (1967): Anandite, a new barium iron silicate from Wilagedera, North Western Province, Ceylon. *Mineral. Mag.* **36**, 1-4.

RIEDER, M., CAVAZZINI, G., D'YAKONOV, Y.S., FRANK-KAMENETSKII, V.A., GOTTARDI, G., GUGGENHEIM, S., KOVAL', P.V., MÜLLER, G., NEIVA, A.M.R., RADOSLOVICH, E.W., ROBERT, J.-L., SASSI, F.P., TAKEDA, H., WEISS, Z. & WONES, D.R. (1998): Nomenclature of the micas. *Can. Mineral.* **36**, 905-912.

SHANNON, R.D. (1976): Revised effective ionic radii and systematic studies of interatomic distances in halides and chalcogenides. *Acta Crystallogr.* **A32**, 751-767.

SHELDRICK, G.M. (1997): SHELX*97*. Program for the solution and refinement of crystal structures. University of Göttingen, Göttingen, Germany.

________ (1998): SADABS *User Guide*. University of Göttingen, Göttingen, Germany.

SOLIE, D.N. & SU, SHU-CHUN (1987): An occurrence of Ba-rich micas from the Alaska Range. *Am. Mineral.* **72**, 995-999.

WENDLANDT, R.F. (1977): Barium-phlogopite from Jaystack Butte, Highwood Mountains, Montana. *Carnegie Inst. Wash. Year Book* **76**, 534-539.

YOSHII, M., MAEDA, K., KATO, T., WATANABE, T., YUI, S., KATO, A. & NAGASHIMA, K. (1973a): Kinoshitalite, a new mineral from the Noda–Tamagawa mine, Iwate Prefecture. *Chigaku Kenkyu* **24**, 181-190 (in Japanese).

________, TOGASHI, Y. & MAEDA, K. (1973b): On the intensity changes of basal reflections with relation to barium content in manganoan phlogopite and kinoshitalite. *Bull. Geol. Surv. Jap.* **24**, 543-550.

Received July 26, 2004, revised manuscript accepted May 1, 2005.